Check for updates

On line kinetic analysis of permeation profiles for UV filter loaded microemulsions using an automatic system with spectroscopic detection and a chemometric approach†

Danielle Silva do Nascimento,‡ Verónica Volpe,‡ Matías Insausti and Marcos Grünhut [ID] *

The analysis of the permeation kinetics of new UV filter formulations is of great importance since the kinetic parameters are related to the effectiveness of the product over time. The dynamics of this process can be evaluated by means of the calculation of the permeation kinetic constants, which can be obtained from the respective permeation profiles. This paper is aimed at improving the analytical performance of permeation assays using an on-line automatic system with spectrometric detection avoiding the chromatographic procedure and the usually manual sampling steps required using the traditional Franz diffusion cell. Then, the kinetics of permeation of octyl *p*-methoxycinnamate loaded in different microemulsions through a synthetic membrane (polyamide) was analysed at real time by UV-Vis and fluorescence spectroscopies. The spectral data were obtained at regular intervals of time (5 min) during 60 min, and the concentration of the permeated UV-filter was at each time calculated using univariate linear calibration. The interference caused by the presence of basil essential oil (oily phase) in some microemulsion samples was overcome using synchronous fluorescence spectroscopy ($\Delta\lambda = 60$ nm) and partial least squares. In all cases, the permeation profiles were obtained (first-order kinetics) and the respective permeation kinetic constants were calculated. The validation of the proposed method was assessed by gas chromatographic-mass spectroscopy and non-significant differences for the obtained permeation kinetic constants were found between methods ($p = 0.05$). Additionally, a commercial sample was analysed with the proposed methods and the results were validated by high performance liquid chromatography technique.

Introduction

UV filters are incorporated in sunscreens in order to protect the skin from damage caused by UV radiation.[1,2] These formulations are usually applied superficially to large skin areas. Therefore, the effectiveness of the filters relies on the level of adhesion of the preparations on the skin[3,4] and the subsequent permeation of the protective film.[5] Octyl *p*-methoxycinnamate (OMC) is a UV-B filter (290–320 nm) widely used in personal care products and represents one of the most common liposoluble absorbers incorporated in sunscreen formulations.[6,7] The behaviour of OMC in different formulations has been well studied due to the fact that a photoisomerization processes can occur and affect the UV-B filtering efficacy of the final product.[8]

INQUISUR (UNS-CONICET), Department of Chemistry, Universidad Nacional del Sur, Av. Alem 1253, Bahía Blanca, B8000CPB, Argentina. E-mail: mgrunhut@uns.edu.ar

‡ These authors contributed equally to the work.

In recent years, colloidal drug carriers including polymeric nanocapsules,[9] lipid nanoparticles,[10] solid lipid nanoparticles[11] and emulsions,[12,13] have attracted an increasing interest as potential OMC carriers. In addition, different studies have proposed the microemulsions as a new generation of OMC carriers.[14–16]

Microemulsions (MEs) are used in the pharmaceutical field, since they can be used in dosage systems or as drug release vehicles that can be administered *via* oral, parenteral or topical.[17] ME systems are mixtures composed of surfactant, co-surfactant, water and oil, and are optically isotropic and thermodynamically stable.[18,19] MEs have the ability to stabilize lipophilic compounds, as well as achieving a high applicability and bioavailability of the active substances. In case of lipophilic compounds, oil-in-water (o/w) microemulsions are preferred, especially when the active substance is used for topical applications.[9,20]

In the pharmaceutical and cosmetic field, the *in vitro* release studies are effectively employed for permeation, release and dissolution testing as part of the quality control of the

pharmaceutical formulations.[21] Hence, transdermal permeability studies of active substances are performed using the Franz diffusion cell.[22–24] Briefly, this cell consists of a donor and an acceptor compartment, which are separated by a membrane. The donor compartment keeps the drug formulation and the acceptor compartment contains the media receptor that emulates the physiological condition of the skin. This solution should be always mixed with a magnetic bar to ensure a uniform diffusion process and homogeneity of concentration. Due to the fact that the diffusion phenomenon depends on the temperature, the cell is kept at constant temperature by means of a thermostated water bath. While the experiment is performed, the samples are taken from the acceptor medium by means of the Franz cell sampling tube and analysed at regular intervals of time. The permeation study is laborious and it involves the control of the temperature, stirring and a series of manual steps. Moreover, when the analysis of the sample is performed by a chromatographic procedure, the method does not provide real-time information since it requires a long time of analysis. Additionally, the use of hazardous organic solvents of high purity is required.

The use of automatic methods with on-line UV-Vis and/or fluorescence detection can be considered an alternative to overcome several of the mentioned problems.[25] These systems allow real-time monitoring; provide a higher sampling frequency and the replacement of laborious and tedious manual procedures.[14,15] UV-Vis spectroscopy (UVS) and fluorescence spectroscopy (FS) are distinguished techniques since they are fast, simple, cheap, and require little or no pretreatment of samples.[26–29] Synchronous fluorescence spectroscopy (SFS) has been successfully applied in the determination of different components in presence of interferences since it allows simultaneous scanning of the excitation and emission wavelengths while maintaining a constant difference between these two wavelengths ($\Delta\lambda$).[30] In this way, SFS reduces spectral overlaps narrowing spectral bands and simplifies spectra.[31] Moreover, the combined use of chemometrics and SFS is presented as a powerful analytical alternative since it generates accurate calibration models that allow the simultaneous determination of multiple analytes in presence of unknown interferences, even in cases in which the selectivity is poor. In this sense, partial least squares (PLS) is a multivariate calibration technique that performs data decomposition in spectral *scores* and *loadings* matrices prior to model building with the aid of these new variables.[32] SFS and PLS have been used together in many analytical applications.[33,34] However, few reports showing the application of these methods in the study of microemulsion based samples have been published.[35]

This work aims to propose an on line automated system based on the use of the Franz diffusion cell to obtain the permeation kinetic constants of OMC in lab-synthesised microemulsions and emulsion commercial samples. The use of UVS and FS techniques allowed monitoring the OMC permeation process at real-time through a polyamide membrane, which simulates the skin. Additionally, the SFS technique assisted by PLS allowed obtaining permeation kinetic profiles and permeation kinetic constants in presence of

interference signals. The proposed methods were successfully validated by chromatographic techniques.

Experimental section

Materials and software

All reagents were analytical-grade chemicals and ultra-pure water (18 MΩ cm^{-1}) was obtained from a Barnsted® water purification system. Decaethylene glycol mono-dodecyl ether (DME; Sigma-Aldrich®) and ethyl alcohol (ET; Dorwil®) were used as non-ionic surfactant and co-surfactant, respectively. Oleic acid (OA; Applichem®) and *Ocimum basilicum* essential oil (BEO; Euma®) were used as oily phase and octyl *p*-methoxycinnamate (OMC; Sigma-Aldrich®) was used as UVB filter.

A mixture of distilled water and absolute ethanol (1 : 1 v/v) was used as the acceptor solution (AS). Stock solutions of OMC and BEO were prepared by dissolving 0.0600 g of OMC and 0.0600 g of BEO in 10 mL of AS, respectively. Working solutions were prepared by appropriate dilution of stock solution with AS. Whatman® polyamide membranes (PA) were used for tests and presented a pore size of 0.45 μm.

A commercial emulsion containing OMC (Dermaglós®) was purchased from a local pharmacy (Bahía Blanca, Argentina). The preparation of the sample for subsequent analysis was carried out dissolving 0.5000 g of emulsion in 50 mL of ethanol. Then, 1 mL of this dissolution was diluted up to 50 mL with ethanol.

PLS calculations were performed by means of a lab-made routine written in MatLab® 2010a software. The computer programme used to control the automatic system was developed using the open-source Arduino software (IDE, 1.0.x).

Methods

Preparation of OMC loaded o/w microemulsions. Two OMC loaded microemulsions (OMC-MEI and OMC-MEII) were analysed and obtained as described in previous reports (Nascimento *et al.*[14] and Volpe *et al.*,[15] respectively) using biocompatible materials. In both cases, appropriate concentrations of OMC were chosen according to the technical specifications of the Food and Drug Administration (US) and the European Union, which authorize a maximum concentration of 7.5% (w/w) and 10.0% (w/w) of OMC, respectively. In all cases, the mixtures were visually examined in order to evaluate the degree of transparency and stored in amber-glass containers at room temperature (25 °C).

Preparation of OMC-MEI samples. OMC-MEI was formed by OA as oily phase and a 3 : 1 mixture of DME : ET (surfactant : co-surfactant) named SI$_{mix}$. First, the OMC was incorporated into the oily phase by stirring at 25 °C. Then, this mixture was added to the SI$_{mix}$ and titrated with ultra-pure water under moderate magnetic stirring. The obtained final concentrations of DME, ET, OA and OMC in OMC-MEI were: 21.9, 7.3, 1.5 and 5.0% (w/w), respectively.

Preparation of OMC-MEII samples. OMC-MEII was formed by BEO as oily phase and a 2 : 1 mixture of DME : ET (surfactant : co-surfactant) named SII$_{mix}$. Briefly, the OMC was

incorporated into the oily phase by stirring at 25 °C and this mixture was added to the SII_{mix} and titrated with ultra-pure water under moderate magnetic stirring. The obtained final concentrations of DME, ET, BEO and OMC in OMC-MEII were: 19.3, 9.7, 6.0 and 1.5% (w/w), respectively.

Physico-chemical characterization of OMC-MEI and OMC-MEII samples. A series of assays were carried out in order to verify the physicochemical properties of the obtained OMC loaded microemulsions. Average droplet size (Z) and poly-dispersity index (PdI) were determined by dynamic light scattering (DLS) using a Malvern® Zetasizer Nano Series equipment. Therefore, 5.00 g of sample (OMC-MEI or OMC-MEII) was dispersed in 50 mL of ultra-pure water and the obtained dispersion was then stirred during 2 h at 25 °C. The measurements were performed at room temperature and at a 90° angle. Moreover, the pH measurements were performed by using an Orion model 710A pH meter with an Orion-Ross® model 81-02 electrode.

On-line automatic system for *in vitro* permeation study. The permeation study with on-line detection was performed using an automatic continuous flow system coupled to a traditional Franz diffusion cell (Fig. 1). The diffusion area of the Franz diffusion cell (Glass workshop, Department of Chemistry, Universidad Nacionaldel Sur) was 3.14 cm^2. A PA was placed between the two compartments (donor and acceptor), which was previously submerged in the AS for 24 h. Then, the acceptor compartment was fully filled with 25 mL of AS. This solution was stirred during the experiment (300 rpm) using a magnetic stirrer (Hanna Instruments, HL190M). The Franz diffusion cell was thermostated by means of a circulating water bath system (Cole Parmer® BT-15) in order to ensure that the temperature was kept at 32.0 ± 0.5 °C on the surface of the PA. Additionally, the cell was enveloped in aluminium foil to prevent the photodegradation of OMC. The sample (0.1000 g) was initially placed in the donor compartment in contact with the membrane and at that moment the permeation process started. Then, 100 μL of AS were pumped towards the detector (UV or fluorescence) at 0.25 mL min^{-1} by activation of the peristaltic pump (Gilson® Minipuls 3). The peristaltic pump was provided with a Tygon® tube of 0.50 mm i.d. and operated at 13 rpm. The whole permeation analysis lasted 60 min and sampling was

performed every 5 min intervals. It is important to note that the volume of sample aspired at each time must be recovered. For this reason, a volume of 100 μL of AS was aspirated from a flask at 0.25 mL min^{-1} and thrown toward the Franz cell. The microprocessor unit mainly consisted of an Arduino circuit board (AC) model Mega 2560,[36] which controlled the start/stop and speed of the peristaltic pump, the magnetic stirrer, the water bath and the spectra register.

Data acquisition

UV spectra acquisition. The spectral measurements were carried out in an Agilent model HP 8453 UV-Vis spectrophotometer equipped with a quartz cell (Hellma®, 18 μL and 10 mm optical path). The spectra were registered in the range between 190 and 1100 nm with 1 nm resolution. The adjustment of the absorbance signal was performed using the AS as blank.

Fluorescence spectra acquisition. The spectral measurements were carried out in a Jasco model FP-6500 spectrofluorometer. A flow quartz cell (Hellma®, 50 μL) was used in right-angle. The slit width was 5 nm for excitation and 5 nm for emission. The acquisition interval and integration time were maintained at 1 nm and 1.0 s, respectively. The scan rate was 2000 nm min^{-1} and the photomultiplier tube voltage operated at 550 V. An excitation wavelength of 366 nm was selected and the fluorescence emission spectra were collected between 380 and 600 nm.

In the case of SFS, the slit width was 3 nm for excitation and 5 nm for emission. The fluorescence spectra of the samples were recorded within the range of 370–690 nm and keeping a fixed $\Delta\lambda$ (difference between excitation and emission wavelength) of 60 nm. The scan rate was 2000 nm min^{-1} and the photomultiplier tube voltage operated at 550 V. The acquisition interval and integration time were fixed at 0.5 nm and 0.5 s, respectively. Therefore, each spectrum presented 641 values of fluorescence intensity.

Data analysis. The different concentration values of OMC in the AS during the permeation study were calculated every 5 min during 60 min. In the case of OMC-MEI samples, the concentration of OMC was calculated at each time by univariate linear calibration. A set of six standard solutions was prepared in the concentration range of 6.0 and 60.0 mg L^{-1} of OMC. These
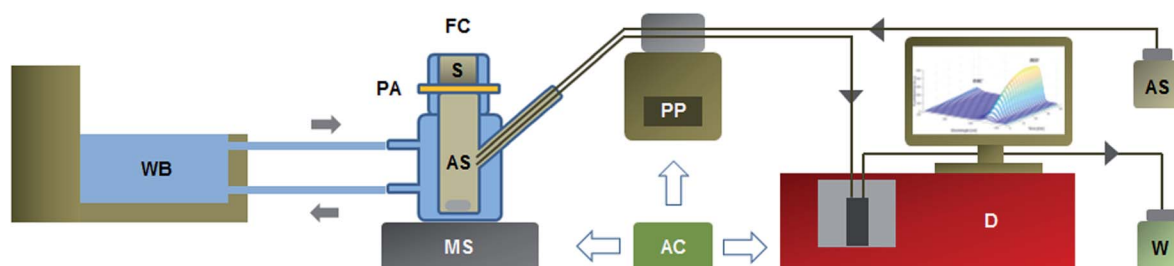

Fig. 1 Automatic continuous flow system coupled to a Franz diffusion cell for *in vitro* permeation study with on-line spectrometric detection. AC: Arduino circuit board; AS: acceptor solution (water : ethanol (1 : 1 v/v)); D: detector (UV: 340 nm, fluorescence: 390 nm, synchronous fluorescence: $\Delta\lambda = 60$ nm; 370–690 nm); FC: Franz diffusion cell; MS: magnetic stirrer (300 rpm); PA: polyamide membrane (3.14 cm^2); PP: peristaltic pump (13 rpm); S: sample (0.1000 g); W: waste; WB: water bath (32.0 °C). The arrows indicate the direction of fluids (0.25 mL min^{-1}). The whole permeation analysis lasted 60 min and sampling was performed every 5 min intervals.

values were established considering the concentration of the OMC in the samples. In the case of OMC-MEII samples, the cumulative amount of OMC permeated through the membrane was calculated implementing PLS due to the fact that BEO (oily phase) fluorescence signal generated interference on the OMC signal. Thus, a full factorial experimental design 3^2 was used. Different concentrations of OMC (6.0 to 60.0 mg L^{-1}) and BEO (24.0 to 240.0 mg L^{-1}) were prepared in the AS (Table S1†). Briefly, PLS regression is a calibration technique that generalizes and combines the characteristics of principal component analysis (PCA) and multiple linear regression (MLR).[32] The prediction is achieved by calculating a new small set of vectors that result from the obtained spectra called *latent variables* or *loadings*. A new set of values called *scores* is also calculated for all the samples using these latent variables. By using the scores, it is possible to obtain a linear calibration model that can be later used for the prediction of the concentration of a compound in unknown samples. A full cross validation process is necessary in order to select the best number of latent variables used in each model. Hence, the performance of the obtained PLS models is evaluated by the calculation of the root mean square error of prediction (RMSEP) and the relative error of prediction (REP) calculated as:

$$\text{RMSEP} = \left[\frac{\sum_{n=1}^{n} \left(C_{\text{nom}} - C_{\text{pred}} \right)^2}{n} \right]^{1/2} \quad (1)$$

where C_{nom} and C_{pred} represent the nominal and predicted concentrations, respectively, and I is the total number of samples.

$$\text{REP} = \frac{100}{C_{\text{mean}}} \left[\frac{\sum_{n=1}^{n} \left(C_{\text{nom}} - C_{\text{pred}} \right)^2}{n} \right]^{\frac{1}{2}} \quad (2)$$

where C_{mean} is the mean concentration (*i.e.* the central point in the experimental design). In addition, the models can be evaluated in terms of sensitivity (SEN) and limit of detection (LOD) calculated as follows:

$$\text{SEN}_k = \frac{1}{b_k} \quad (3)$$

where the denominator is the Euclidean norm of the vector b_k, which is the vector of the regression coefficients obtained for component k.

$$\text{LOD}_k = 3.3 \delta r b_k \quad (4)$$

where δr indicates the instrumental noise.

GC-MS analysis. The determination of OMC at each time during the permeation process was also performed by gas chromatography-mass spectrometry (GC-MS) using an Agilent GC model 7890B gas chromatography coupled to a 5977A mass spectrometer. The system was equipped with a fussed silica capillary HP-5 column (30 m × 0.25 mm i.d.; film thickness 0.25 µm). The inlet temperature was 290 °C and the injected volume

was 1 µL using the split mode (split ratio: 20/1). Helium was used as the carrier gas at a flow rate of 1.0 mL min^{-1}. The oven was programmed in order to increase the temperature from 40 to 100 °C (3 °C min^{-1}) and later up to 280 °C (10 °C min^{-1}). Then, the oven temperature was kept at 280 °C for 5 min. The ion source and MS transfer line temperature were set to 230 °C and 260 °C, respectively. The mass spectrometer was operated in electron impact mode (EIM) at 70 eV.

Under these conditions, the retention time (t_R) of OMC was 17.4 min. The fragments of the analyte were monitored by selecting the ion monitoring mode (SIM). Thereby, the ions (m/z) used in the analysis of the compound of interest were 290, 178 and 161. The calibration of the method was carried out by preparing a series of OMC standard solutions of concentrations in the range of 6.0–48.0 mg L^{-1}.

HPLC analysis. An HPLC Thermo Fisher Scientific model Ultimate 3000-MSQ PLUS system equipped with an Acclaim™ 120 C18 reverse phase column (3 µm particle size, 2.1 mm × 150 mm) was used for the quantification of OMC in the commercial sample at each sampling time during the permeation process. OMC was monitored with the use of a UV detector at 311 nm. The mobile phase was controlled by the activation of binary pumps at 25 °C and the flow rate was 0.2 mL min^{-1}. The mobile phase consisted of methanol and ultrapure water in an 85 : 15 (v/v) ratio. In addition, isocratic mode was used and the injected sample volume was 20 µL. An external calibration curve was constructed using standard solutions of OMC in the range of 6.0–60.0 mg L^{-1}. The peak area obtained for a retention time of 16.0 min was employed for the OMC quantification.

Results and discussion

Obtention and characterization of OMC-MEs

The prepared o/w microemulsions resulted in homogeneous and transparent systems which allowed the solubilization of a non-polar substance as OMC in their oily phase.[19] In Table 1 the composition of OMC-MEI and OMC-MEII samples and the parameters obtained by DLS technique are shown. In both cases, Z values indicate a droplet size in nanometric scale[37] and the PDI values demonstrating that the obtained

Table 1 Percentage composition and results of the physicochemical characterization corresponding to the synthesised OMC loaded o/w microemulsions. The measurements were performed in triplicate

	S_{mix} (%)	OA (%)	BEO (%)	Water (%)	OMC (%)
OMC-MEI	29.2	1.5	—	64.3	5.0
OMC-MEII	29.0	—	6.0	63.5	1.5

	Z (nm)	PdI	C (mS cm^{-1})	pH	IR
OMC-MEI	11.91 ± 0.09	0.191 ± 0.029	0.116 ± 0.020	5.72 ± 0.04	1.35 ± 0.02
OMC-MEII	12.60 ± 0.10	0.389 ± 0.042	0.045 ± 0.003	4.91 ± 0.03	1.37 ± 0.01

microemulsions tend to approach monodisperse systems and become stable systems due to the uniformity in the drops.[38] Additionally, the particle size distribution histogram obtained through DLS measurements on the OMC loaded o/w microemulsions is shown in Fig. S2.† On the other hand, the conductivity values of OMC-MEI and OMC-MEII were in the range of 0.045 to 0.116 mS cm^{-1} showing that all the obtained microemulsions were oil in water type. The refractive index measured values were in the range of 1.35 and 1.37, which indicates that the obtained microemulsions were isotropic systems. Regarding the pH, both OMC-MEI and OMC-MEII samples presented values that indicate that they are suitable for topical use. Additionally, the microemulsions were stable during the storage and along the analysis (20–35 °C).

Permeation study

The permeation process of OMC in the case of the synthetized microemulsions (OMC-MEI and OMC-MEII) was optimized and evaluated at real time using the proposed automatic system with spectrometric detection (UV and/or fluorescence). For that purpose, different methods to quantify OMC in the analysed samples were developed and the concentration profiles were obtained. Finally, the kinetic constants corresponding to the permeation process were calculated for each formulation and the dynamics of diffusion was then discussed. Additionally, a commercial sample containing OMC was analysed. The proposed methods were validated by GC-MS and HPLC techniques.

Experimental conditions

As mentioned before, in Franz's cell the donor compartment maintains the formulation and the acceptor compartment contains the AS. OMC is a hydrophobic compound (log P = 5.96) insoluble in water (<0.1 g/100 mL at 27 °C). However, OMC is miscible in alcohols, propylene glycol, and various oils. For this reason, a 1 : 1 (v/v) mixture of distilled water and absolute ethanol was chosen as the acceptor fluid in the study because of the high solubility of OMC in ethanol. On the other hand, the membrane that separates both compartments (donor and acceptor) should behave in a similar way to skin, allowing the active compound to diffuse to the acceptor medium. A previous report showed that polyamide membranes can be adequate for lipophilic compounds due to the fact that they offer minimal rate-limiting effects and present an adequate size exclusion pore, allowing only net translocation of the interest compound from the formulation into the receptor compartment.[39] Therefore, these synthetic membranes can be seen as an alternative to human or animal skin when evaluating OMC topical permeation, reducing cost and time.

Regarding the temperature, it is known that the diffusion phenomenon depends on this variable. In our case, the analysis was performed at 32 °C, a normal value for human skin.[40] Moreover, uniformity and homogeneity of AS during the permeation process were achieved by stirring.

On-line automatic system

The permeation process of OMC in the analysed samples was monitored using the automatic system described in the section: *on-line automatic system for in vitro permeation study*. The hydrodynamic variables of the system were optimized. The flow rate was studied between 0.10 and 0.40 mL min^{-1} and the optimal value was 0.25 mL min^{-1}. This rate allowed the register of the UV and fluorescence spectra at the required time intervals (5 min) since it only took 24 s to aspirate 100 μL of sample. The same flow rate (0.25 mL min^{-1}) was used to recover with AS the volume of sample (100 μL) thrown towards the detector at each sampling time. This step was performed simultaneously to the aspiration of the sample in a way that the total volume of AS in the Franz's cell remained constant. The components of the on-line system (peristaltic pump, water bath, magnetic stirrer and detectors) were fully commanded by Arduino which is an open-source electronics platform based on easy-to-use hardware and software. The proposed system offers advantages compared to the traditional batch procedure such as automatic sampling, temperature control, stirring and on-line signal detection allowing the real time monitoring of the permeation process. These features contribute to decrease the possible risks of human errors and shorten the time of analysis in comparison to manual sampling and chromatographic determination frequently used for this kind of analysis.

Spectrometric detection

UV detection. In Fig. 2a the UV molecular absorption spectra of the pure components corresponding to the OMC-MEI formulation, that is, the oily phase (OA) and the OMC chemical filter are shown at their corresponding concentrations (1.5% and 5.0% (w/w), respectively). As it can be observed, there is a strong absorption around 280 nm for OA and at 340 nm for OMC. However, at wavelengths around 340 nm, OA practically does not absorb radiation. Thus, OMC was determined using the univariate linear calibration method. As was mentioned in section UV-Vis spectra acquisition, the calibration curve included six points with three replicates for the OMC determination over the range of 6.0–60.0 mg L^{-1}. The equation of the regression line obtained for UV detection was $A = (0.021 \pm 0.001)$ [OMC (mg L^{-1})] + (0.029 ± 0.003), with a correlation coefficient of 0.994. The sensitivity was evaluated as a limit of detection (LOD) and limit of quantification (LOQ), and the obtained values were 0.05 mg L^{-1} and 0.14 mg L^{-1}, respectively. In the case of OMC-MEII formulation, in Fig. 2b the UV spectra of the pure components, that is BEO (oily phase) and OMC are shown at concentrations of 6.0% and 1.5% (w/w), respectively. It can be observed that an important spectral overlapping between both species throughout the analysed region exists. Therefore, it was not possible to quantify OMC using UVS for the OMC-MEII formulation due to the strong interference presented by BEO around 340 nm.

Fluorescence detection. As mentioned before, OMC presents molecular fluorescence when it becomes excited at 366 nm. In Fig. 3 the fluorescence spectrum corresponding to a standard solution of OMC (30.0 mg L^{-1}) is shown and it can be observed
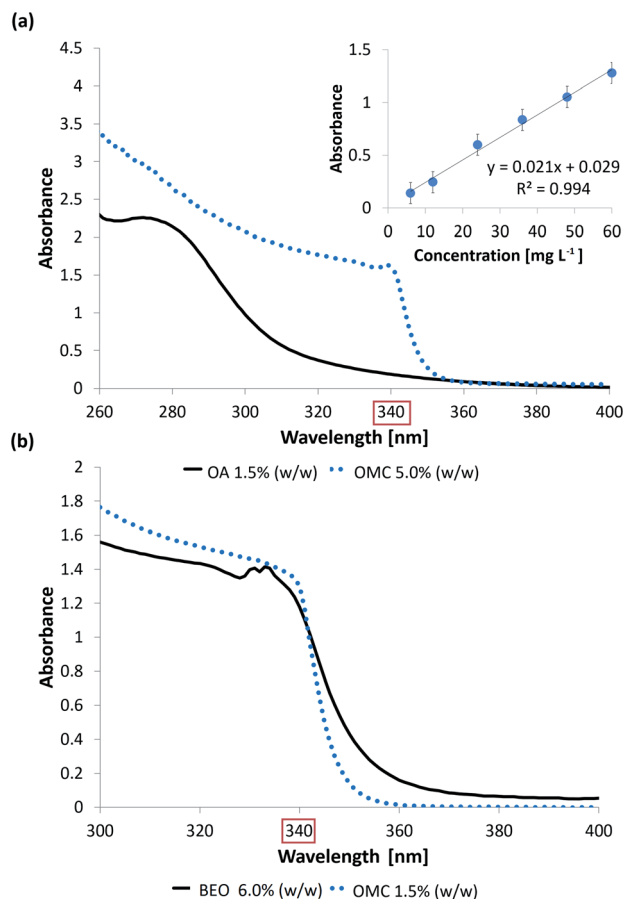
Fig. 2 (a) UV absorption spectra of a 1.5% (w/w) OA standard solution (black solid line) and a 5.0% (w/w) OMC standard solution (blue dotted line). The calibration curve for OMC at 340 nm and in the concentration range of 6.0–60.0 mg L^{-1} is also shown. (b) UV absorption spectra of a 6.0% (w/w) BEO standard solution (black solid line) and a 1.5% (w/w) OMC standard solution (blue dotted line).

the characteristic maximum of signal at 390 nm. Since OA is not fluorescent around 390 nm, in the case of OMC-MEI formulation it was possible to quantify OMC by univariate linear
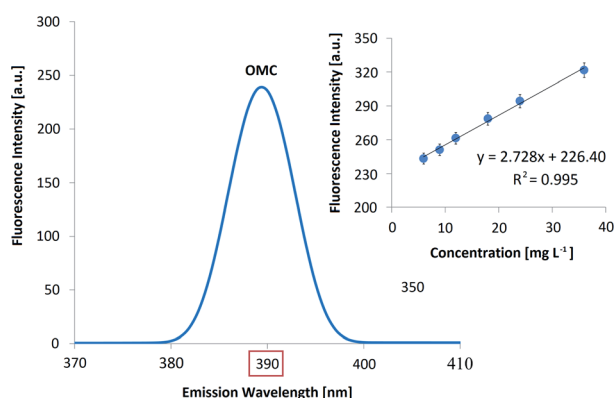

Fig. 3 Fluorescence spectrum corresponding to a standard solution of OMC (30 mg L^{-1}). The characteristic maximum of signal at 390 nm and the calibration curve in the concentration range of 6.0–36.0 mg L^{-1} are shown. It is important to note that OA is not fluorescent around 390 nm.

calibration. Then, a calibration curve was constructed over the linear range of 6.0–36.0 mg L^{-1} that included six points with three replicates each. The resulting regression equation was $I = (2.728 \pm 0.019)$ [OMC mg L^{-1}] + (226.40 ± 0.02) with a correlation coefficient of 0.995. The LOD and LOQ obtained values were 0.08 mg L^{-1} and 0.24 mg L^{-1}, respectively.

Regarding the OMC-MEII formulation, the oily phase (BEO) generated interference in the OMC fluorescence spectra. At first, the resolution of the OMC and BEO bands was improved applying SFS. The registered fluorescence spectra as a function of permeation time corresponding to the central point of the experimental design are shown in Fig. 4a. It can be observed that the emission band between 370 and 420 nm corresponds to OMC while the band between 570 and 650 nm corresponds to BEO.

However, the spectral analysis of mixtures with a high BEO : OMC ratio showed that the fluorescence signal intensities corresponding to OMC band can be affected in presence of BEO. To overcome this problem, PLS algorithm was applied to the spectral data corresponding to the proposed experimental design. In Fig. 4b the first latent variable calculated is shown and it corroborates the interference in the fluorescence signals between BEO and OMC. In this way, PLS algorithm allowed obtaining calibration models for both BEO and OMC. In the
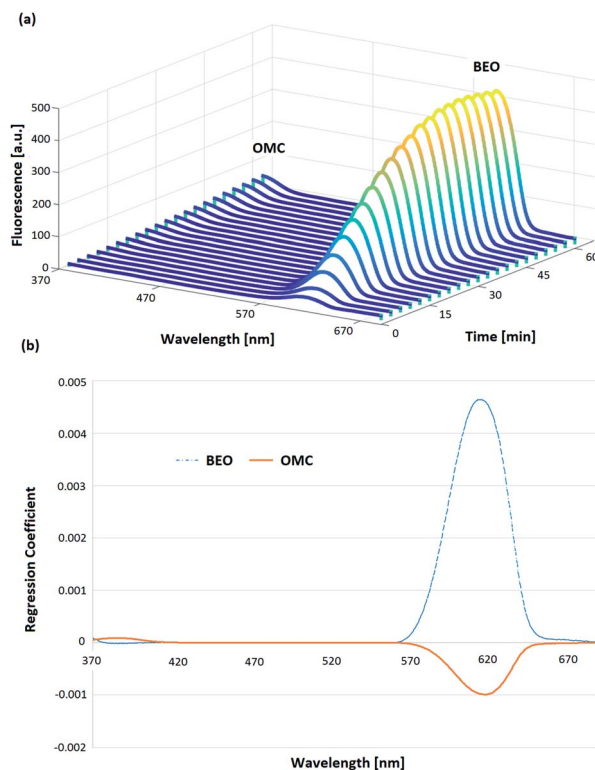

Fig. 4 (a) Synchronous fluorescence spectra (370–690 nm) corresponding to the central point of the experimental design registered as function of the permeation time (60 min). The emission band between 370 and 420 nm corresponds to OMC while the band between 570 and 650 nm corresponds to BEO. (b) First latent variable for PLS models corresponding to OMC (orange solid line) and BEO (blue dotted line).

case of BEO calibration only two new variables were required to explain 98.4% of variance. In the case of OMC calibration, three latent variables were necessary to explain 97.5% of the variance. The need for a higher number of variables to obtain a good prediction can be explained due to the fact that the BEO signal is more intense than the one corresponding to OMC, consequently it was more difficult to explain the interaction between each other. The analytical performance for BEO and OMC calibration models is shown in Table 2. Optimal predictions were reached for both models, obtaining a low REP and an acceptable determination coefficient (R^2) in each case. Moreover, the LOD and LOQ values were optimal taking into account the expected concentrations at each sampling time during the permeation process. Hence, a PLS model was used to predict the concentration of OMC at different permeation times from SFS data obtained with the proposed automatic method.

GC-MS method. The permeation of OMC for OMC-MEI and OMC-MEII formulations was also monitored by GC-MS in order to validate the proposed methodology. In Fig. S3† the chromatogram indicating the peak of OMC at a retention time of 17.4 min is shown. A calibration curve was constructed and the resulting regression equation was $I = (6.33 \times 10^4 \pm 4.12 \times 10^2)$ [OMC mg L^{-1}] $- (5.00 \times 10^6 \pm 4.12 \times 10^3)$. The method provided good linearity ($R^2 = 0.993$) over a concentration range of 6.0–48.0 mg L^{-1}.

Obtention of permeation profiles

The spectrometric methods allowed calculating the different values of concentrations of OMC in the AS throughout the permeation process and afterwards the obtention of the respective permeation profiles. These profiles are curves that represent how the concentration of an active substance diluted in the receptor medium varies as a function of the permeation time after passing through a membrane. In Fig. 5a and b the permeation profiles corresponding to OMC-MEI and OMC-MEII formulations are shown, respectively. In the first case, three permeation profiles were obtained since UV-Vis, fluorescence and GC-MS methods were used for the quantification of OMC during the permeation process. In the case of OMC-MEII formulation, two permeation profiles were obtained, since SFS
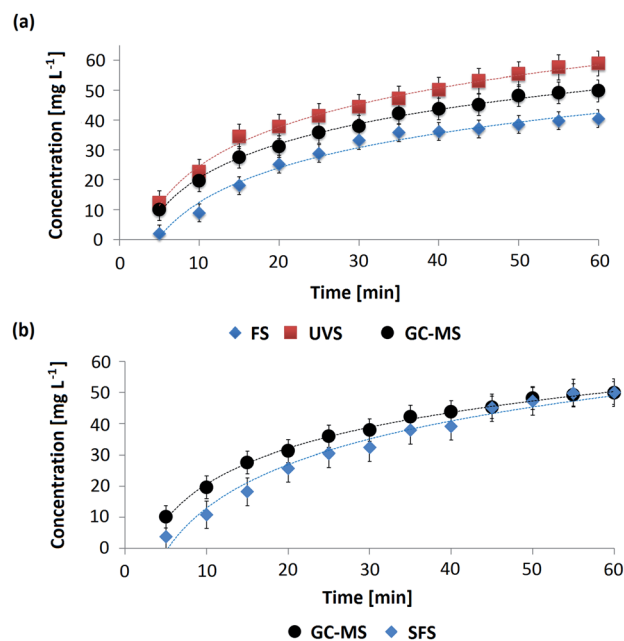

Fig. 5 Permeation profiles for OMC in the o/w microemulsions obtained using the proposed methodology and the reference method. (a) OMC permeation profiles corresponding to OMC-MEI obtained by UVS (red squares), FS (blue diamond) and GC-MS (black circle) methods. (b) OMC permeation profiles corresponding to OMC-MEII obtained by SFS (blue diamond) and GC-MS (black circle) methods. The experiments were performed in triplicate.

and GC-MS quantification methods were applied. It can be observed, the formulations exhibited an increase in OMC permeation up to 60 min followed by a constant permeability through the membrane. In Table S4† the fitting functions for the different permeation profiles and their respective R^2 values are shown. In all cases, these results indicate that the permeation of OMC follows zero-order kinetics.

Kinetic constants calculation

Considering that OMC followed zero-order kinetics in both OMC-MEI and OMC-MEII formulations, the calculation of the

Table 2 Analytical parameters corresponding to PLS models used for the determination by SFS of OMC and BEO during the permeation process of OMC-MEII formulation. Also, the determination coefficients (R^2) corresponding to the kinetic models and the permeation kinetic constants (K_p) of OMC and BEO are shown. The experiments were performed in triplicate

		OMC	BEO
PLS models	Spectral range (nm)	370–650	
	Concentration range (mg L^{-1})	6.0–60.0	24.0–240.0
	Latent variables	3	2
	RMSEP (mg L^{-1})	3.52	17.90
	REP (%)	6.51	8.30
	R^2	0.975	0.959
	LOD (mg L^{-1})	1.31	2.79
	LOQ (mg L^{-1})	3.97	8.48
	SEN (L mg^{-1})	1.98	4.12
Kinetic models	R^2 (zero-order kinetics)	0.952	0.966
	K_p (cm min^{-1})	$2.98 \times 10^{-4} \pm 5.33 \times 10^{-5}$	$4.82 \times 10^{-4} \pm 4.06 \times 10^{-5}$

Table 3 Permeation kinetic constants (K_p) of OMC in OMC–MEI and OMC–MEII formulations obtained by the proposed methods (UVS, FS and SFS) and the reference method (GC–MS). The measurements were performed in triplicate

OMC-MEI	UVS	FS	GC-MS
K_p (cm min^{-1})	$1.21 \times 10^{-4} \pm 1.76 \times 10^{-6}$	$1.65 \times 10^{-4} \pm 3.29 \times 10^{-5}$	$1.14 \times 10^{-4} \pm 1.38 \times 10^{-5}$
$t_{calculated}$	1.07	3.03	—
$t_{critical}$ [a]	3.18		

OMC-MEII	UVS	SFS	GC-MS
K_p (cm min^{-1})	—	$2.98 \times 10^{-4} \pm 5.33 \times 10^{-5}$	$2.07 \times 10^{-4} \pm 1.47 \times 10^{-5}$
$t_{calculated}$	—	3.12	—
$t_{critical}$ [a]	3.18		

[a] Tabulated 95% confidence limit ($n = 3$).

permeability kinetic constants (K_p) could be carried out using the eqn (5):

$$K_p = \frac{Q}{At(C_0 - C_i)} \tag{5}$$

where Q (mg) is the amount of compound transported through the membrane in the time t (min), A is the exposed area of the membrane expressed in cm^2, and C_0 (mg L^{-1}) and C_i (mg L^{-1}) are the concentrations of the compound on the donor and the receptor solution, respectively. Generally, C_0 is considered the donor concentration and C_i as 0.[20,41] The K_p values calculated using the proposed and the validation methods for the analysed samples are showed in Table 3. Based on the t-test results, we can conclude that there are no statistically significant differences between the K_p values obtained by the proposed methods (UVS, fluorescence and SFS) and those obtained by GC-MS ($\alpha = 0.05$; $n = 3$).

It is important to note that the kinetics of permeation depends on the affinity of the active substance for the components of the formulation. In this sense, a greater release of the active is expected when there is less affinity of the compound for the oily phase. Due to the lipophilic nature of OMC and its high affinity for OA and BEO (oily phases) a relatively slow permeation rate of the active sunscreen would be expected. This fact was corroborated analysing a sample of OMC in an oil-free medium (ethanol : water in a 1 : 1 (v/v) ratio). In this case, the obtained K_p was 5.83×10^{-4} cm min^{-1} corroborating that the

oily components of the microemulsions systems contributed to decrease the permeation rate of OMC. Thus, the analysed formulations (OMC-MEI and OMC-MEII) could help to provide a sustained photoprotection for the skin. However, the permeation rate of OMC in the case of OMC-MEI was lower than the one corresponding to OMC-MEII showing that the tested formulation with OA as internal phase presents a retention effect of OMC for a longer time since a higher affinity for the polyamide membrane occurs.

Since the concentration of BEO could be obtained from SFS data assisted by PLS algorithm, the kinetic permeation constant for BEO was also calculated (4.82×10^{-4} cm min^{-1}). It can be observed, that BEO presented a higher permeation rate with respect to OMC. This information is very useful considering the potential repellent and anti-inflammatory properties that presents the BEO in the OMC-MEII formulation and as previously described by the authors.[15]

Application of the methods in the analysis of a commercial sample

The developed methods based on UV and fluorescence detection were applied in the permeation analysis of a commercial emulsion sample. The obtained K_p values of OMC were compared with the K_p values obtained with the chromatographic method used as reference (in this case, HPLC) and the results are shown in Table 4. Based on the t-test results, there are no statistically significant differences between the K_p values

Table 4 Permeation kinetic constants (K_p) of OMC in a commercial emulsion obtained by the proposed methods (UVS and FS) and the reference method (HPLC). The measurements were performed in triplicate

	UVS	FS	HPLC
R^2	0.987	0.991	0.989
K_p (cm min^{-1})[a]	$8.97 \times 10^{-5} \pm 1.05 \times 10^{-5}$	$9.39 \times 10^{-5} \pm 8.50 \times 10^{-6}$	$1.38 \times 10^{-4} \pm 2.55 \times 10^{-5}$
$t_{calculated}$	2.89	2.82	—
$t_{critical}$ [b]	3.18		

[a] Zero-order kinetics. [b] Tabulated 95% confidence limit ($n = 3$).

Table 5 Comparison of methods developed to *in vitro* permeation studies in different carriers using the Franz diffusion cell[a]

Method	Separation technique	Detection technique	Sample	Automation	Analytes	Membrane	Receptor medium	Solvent
5	HPLC	UVS (310 and 360 nm)	o/w emulsion w/o emulsion	No	OMC BMBM	Cellulose	ET:water (50:50 v/v)	ACN:water (80:20 v/v)
11	HPLC	UVS (310 nm)	o/w emulsion w/o emulsion nanocapsules	No	OMC	Pig skin	BPS/NaCl 120 mM, KCl 2.7 mM, Oramix® 4.0%	ACN:water (85:15 v/v)
42	HPLC	UVS (273 nm)	Lipid nanoparticles	FIA	CF	Pig skin	Hepes buffer	ACN:water (10:90 v/v)
43	No	FS (405 nm)	w/o emulsion	SIA	SA	Polycarbonate	BPS	Not used
44	No	UVS (310 nm)	Liposomes	No	OMC	Cellulose acetate	BPS Polisorbate 80:ET (70:30 v/v)	Not used
This work	No	UVS (340 nm)	o/w microemulsion	CFS	OMC	Polyamide	ET:water (50:50 v/v)	Not used
This work	No	FS (390 nm)	o/w microemulsion	CFS	OMC	Polyamide	ET:water (50:50 v/v)	Not used
This work	PLS	SFS (370-690 nm)	o/w microemulsion	CFS	OMC BEO	Polyamide	ET:water (50:50 v/v)	Not used

[a] UVS: UV-Vis spectroscopy; FS: fluorescence spectroscopy; SFS: synchronous fluorescence spectroscopy; FIA: flow injection analysis; SIA: sequential injection analysis; CFS: continuous flow system; PLS: partial least squares; CF: caffeine; SA: salicylic acid; OMC: octyl *p*-methoxycinnamate; BMBM: butyl-methoxy-di-benzoyl-methane; BEO: basil essential oil; BPS: buffer phosphate solution; ET: ethanol; ACN: acetonitrile.

obtained by both UVS and FS methods with respect to the obtained by HPLC method ($\alpha = 0.05$; $n = 3$). Moreover, it is important to note that the K_p value of the commercial sample is comparable to the obtained for the laboratory synthesised samples (OMC-MEI and OMC-MEII).

Comparison and advantages of the proposed on-line automatic system

Table 5 shows different methods proposed to date in the literature for permeation analysis using the Franz diffusion cell. Recently, Alves *et al.*[42] proposed an automatic method based on flow injection analysis (FIA) for the evaluation of lipid nanoparticles transdermal permeation. However, this method evaluated only caffeine (CF) and it used a chromatographic procedure as a separation technique. Previously, Klimundová *et al.*[43] presented a sequential injection analysis (SIA) system for the permeation study of salicylic acid (SA) in a commercial topical formulation. Although fluorescence detection was used, the permeation of one active substance (SA) in different ointments was addressed. Furthermore, different *in vitro* permeation studies have been carried out for OMC in systems such as o/w emulsions, w/o emulsions, nanocapsules and liposomes. Nevertheless, the automation of the methods was not addressed. Some methods involved HPLC as a separation technique for OMC determination[5,11,42] involving the use of organic solvents during the procedure. In the case of Mota *et al.*,[44] the proposed method did not require a separation technique and OMC permeation was monitored by UV spectrophotometry. It can be concluded that the methods proposed in this work offer the inherent advantages of automation and the use of simple and economic detection techniques as UVS and FS. Moreover, a simple data treatment allowed monitoring two species during the permeation process (OMC and BEO) simultaneously. Moreover, it is important to note that the proposed method is in accordance with several principles of *green analytical chemistry*.[45] In this sense, no organic solvent was used during the determination process and low amounts of waste were generated. Furthermore, the automated method applied reduces human exposure to substances and makes the analytical operation less dependent on the operator.

Conclusions

The proposed on-line methodology with UV and fluorescence detection allowed monitoring at real time the *in vitro* permeation process of the UV filter OMC loaded in o/w microemulsion samples. A highlight of this work was that the interference caused by the oily phase (BEO) in some samples could be overcome using synchronous fluorescence spectroscopy and partial least squares algorithm. In all cases, the permeation process followed zero-order kinetics and the permeation kinetic constants (K_p) for OMC and BEO could be obtained. The K_p values indicated that the OMC loaded in o/w microemulsions presented a lower permeability than the OMC in an oil-free medium. This result suggests that these formulations could promote a more effective action against UV radiation by

remaining on the applied area for a longer period of time. Moreover, the K_p values for the synthetized microemulsions were comparable to the ones obtained for a commercial emulsion sample and were statistically comparable to those obtained by chromatographic procedures (GC-MS and HPLC). The proposed on-line methodology allowed obtaining real-time information, and it was environmental friendly and inexpensive since an automatic flow system coupled to spectroscopic detection techniques was employed avoiding manually sampling, organic solvents and separation techniques. These advantages suggest that the method can be easily implemented in laboratories and can be extended to the study of the permeation process of other active substances even in the presence of interferences.

Conflicts of interest

There are no conflicts to declare.

Acknowledgements

Notes and references

1 A. Chisvert, A. Salvador and M. C. Pascual-Martí, *Anal. Chim. Acta*, 2001, **428**, 183–190.
2 A. Sharma, A. Kumar, C. Li, R. K. Sharma and M. T. Swihart, *RSC Adv.*, 2020, **10**, 34254–34260.
3 S. Songkro, N. L. Lo, N. Tanmanee, D. Maneenuan and P. Boonme, *J. Drug Delivery Sci. Technol.*, 2014, **24**, 703–711.
4 C. Puglia, F. Bonina, L. Rizza, P. Blasi, A. Schoubben, R. Perrotta, M. S. Tarico and E. Damiani, *J. Pharm. Sci.*, 2012, **101**, 301–311.
5 L. Montenegro, R. Turnaturi, C. Parenti and L. Pasquinucci, *Pharmaceutics*, 2018, **10**, 27–40.
6 M. Kanlayavattanakul, N. Kasikawatana and N. Lourith, *J. Cosmet. Sci.*, 2016, **67**, 167–173.
7 L. R. Gaspar and P. M. B. G. Maia Campos, *Int. J. Pharm.*, 2006, **307**, 123–128.
8 C. Couteau, A. Faure, J. Fortin, E. Paparis and L. J. M. Coiffard, *J. Pharm. Biomed. Anal.*, 2007, **44**, 270–273.
9 B. I. Olvera-Martínez, J. Cázares-Delgadillo, S. B. Calderilla-Fajardo, R. Villalobos-García, A. Ganem-Quintanar and D. Quintanar-Guerrero, *J. Pharm. Sci.*, 2005, **94**, 1552–1559.
10 S. Kale, A. Sonawane, A. Ansari, P. Ghoge and A. Waje, *Int. J. Pharm. Pharm. Sci.*, 2010, **2**, 147–149.
11 M. M. Jiménez, J. Pelletier, M. F. Bobin and M. C. Martini, *Int. J. Pharm.*, 2004, **272**, 45–55.
12 A. F. Sierra, M. L. Garduño Ramírez, A. C. Calpena Campmanya, A. R. Martínez and B. C. Naveros, *J. Dermatol. Sci.*, 2013, **69**, 202–214.
13 M. I. R. M. Santoro, D. A. G. C. E. Oliveira, E. R. M. Kedor-Hackmann and A. K. Singh, *Int. J. Pharm.*, 2005, **13**, 197–203.
14 D. S. Nascimento, M. Insausti, B. S. F. Band and M. Grünhut, *Spectrochim. Acta, Part A*, 2018, **191**, 277–282.
15 V. Volpe, D. S. Nascimento, M. Insausti and M. Grünhut, *Colloids Surf., A*, 2018, **546**, 285–292.
16 L. Montenegro, C. Carbone and G. Puglisi, *Int. J. Pharm.*, 2011, **28**, 162–168.
17 M. Fanun, *Curr. Opin. Colloid Interface Sci.*, 2012, **17**, 306–313.
18 P. Boonme, *Journal of Cosmetic Dermatology*, 2008, **6**, 223–228.
19 J. Zhang and B. B. Michniak-Kohn, *Int. J. Pharm.*, 2018, **536**, 345–352.
20 J. Jiesheng, G. Xiaoqiang, H. Xiang and Z. Rongtang, *RSC Adv.*, 2017, **7**, 55360–55363.
21 N. Shiow-Fern, J. J. Rouse, F. D. Sanderson, V. Meidan and G. M. Eccleston, *AAPS PharmSciTech*, 2010, **11**, 1432–1441.
22 L. Montenegro, C. Carbone, G. Condorelli, R. Drago and G. Puglisi, *Drug Dev. Ind. Pharm.*, 2008, **32**, 539–548.
23 A. C. V. Mota, N. M. Volpato, Z. M. F. Freitas and E. P. Santos, *Rev. Cienc. Farm. Basica Apl.*, 2008, **29**, 285–289.
24 M. Alberti, Y. Dancik, G. Sriram, B. Wu, Y. L. Teo, Z. Feng, M. Bigliardi-Qi, R. G. Wu, Z. P. Wang and P. L. Bigliardi, *RSC Adv.*, 2017, **17**, 1625–1634.
25 M. F. Razuc, M. Grünhut, M. Garrido and B. S. F. Band, *Anal. Sci.*, 2014, **30**, 1121–1127.
26 R. P. Stokes and B. L. Diffey, *J. Photochem. Photobiol., B*, 1999, **50**, 137–143.
27 S. Glavanović, M. Glavanović and V. Tomišić, *Spectrochim. Acta, Part A*, 2016, **157**, 258–264.
28 V. K. Rapalli, S. Gorantla, T. Waghule, S. K. Dubey, M. M. Pandey and G. Singhvi, *Spectrochim. Acta, Part A*, 2020, **224**, 117392–117399.
29 R. Ríos-Reina, S. M. Azcarate, J. Camiña and R. M. Callejón, *Food Chem.*, 2020, **323**, 126792.
30 M. Insausti, A. A. Gomes, J. M. Camiña, M. C. U. Araujo and B. S. F. Band, *Spectrochim. Acta, Part A*, 2017, **175**, 185–190.
31 J. R. Lakowicz, *Principles of Fluorescence Spectroscopy*, Baltimore, Maryland, 3rd edn, 2006.
32 S. Wold, M. Sjöström and L. Eriksson, *Chemom. Intell. Lab. Syst.*, 2001, **28**, 109–130.
33 S. Rubio, A. Gomez-Hens and M. Valcarcel, *Talanta*, 1986, **33**, 633–640.
34 A. R. Jalalvand, M. Mahmoudia and H. C. Goicoechea, *RSC Adv.*, 2018, **8**, 23411–23420.
35 F. Pattarino, E. Marengo, M. R. Gasco and R. Carpignano, *Int. J. Pharm.*, 1993, **91**, 157–165.
36 C. A. Squier and B. K. Hall, *J. Invest. Dermatol.*, 1985, **84**, 176–179.
37 F. Salehi, T. Jamali, G. Kavoosi, S. K. Ardestani and S. N. Vahdati, *Int. J. Biol. Macromol.*, 2020, **164**, 3645–3655.
38 K. Kaur, N. K. Bhatia and S. K. Mehta, *RSC Adv.*, 2012, **2**, 8467–8477.
39 S. J. Gallagher, L. Trottet, T. P. Carter and C. M. Heard, *J. Drug Targeting*, 2003, **11**, 373–379.
40 T. J. Franz, *J. Invest. Dermatol.*, 1975, **64**, 190–195.

41 D. B. Hernández, R. K. Mishra, R. Muñoz and J. L. Marty, *Sens. Actuators, B*, 2017, **246**, 606–614.

42 A. C. Alves, I. I. Ramos, C. Nunes, L. M. Magalhães, H. Sklenářová, M. A. Segundo, J. L. F. C. Lima and S. Reis, *Talanta*, 2016, **146**, 369–374.

43 J. Klimundová, K. Mervartová, H. Sklenárová, P. Solich and M. Polásek, *Anal. Chim. Acta*, 2006, **573**, 366–370.

44 A. C. V. Mota, Z. M. F. Freitas, E. R. Júnior, G. M. D. Ortiz, R. Santos-Oliveira, R. A. Ozzetti, A. L. Vergnanini, V. L. Ribeiro, R. S. Silva and E. P. D. Santos, *Int. J. Nanomed.*, 2013, **8**, 4689–4701.

45 A. Gałuszka, Z. Migaszewski and J. Namieśnik, *Trends Anal. Chem.*, 2013, **50**, 78–84.